

Tuning the Excited-State Properties of $[M(\text{SnR}_3)_2(\text{CO})_2(\alpha\text{-diimine})]$ ($M = \text{Ru, Os}$; $R = \text{Me, Ph}$)

Joris van Slageren and Derk J. Stufkens*

Institute of Molecular Chemistry, Universiteit van Amsterdam, Nieuwe Achtergracht 166, NL-1018 WV Amsterdam, The Netherlands

Received August 1, 2000

The influences of R, the α -diimine, and the transition metal M on the excited-state properties of the complexes $[M(\text{SnR}_3)_2(\text{CO})_2(\alpha\text{-diimine})]$ ($M = \text{Ru, Os}$; $R = \text{Ph, Me}$) have been investigated. Various synthetic routes were used to prepare the complexes, which all possess an intense sigma-bond-to-ligand charge-transfer transition in the visible region between a $\sigma(\text{Sn}-\text{M}-\text{Sn})$ and a $\pi^*(\alpha\text{-diimine})$ orbital. The resonance Raman spectra show that many bonds are only weakly affected by this transition. The room-temperature time-resolved absorption spectra of $[M(\text{SnR}_3)_2(\text{CO})_2(\text{dmb})]$ ($M = \text{Ru, Os}$; $R = \text{Me, Ph}$; $\text{dmb} = 4,4'$ -dimethyl-2,2'-bipyridine) show the absorptions of the radical anion of dmb, in line with the SBLCT character of the lowest excited state. The excited-state lifetimes at room temperature vary between 0.5 and 3.6 μs and are mainly determined by the photolability of the complexes. All complexes are photostable in a glass at 80 K, under which conditions they emit with very long lifetimes. The extremely long emission lifetimes (e.g., $\tau = 1.1$ ms for $[\text{Ru}(\text{SnPh}_3)_2(\text{CO})_2(\text{dmb})]$) are about a thousand times longer than those of the $^3\text{MLCT}$ states of the $[\text{Ru}(\text{Cl})(\text{Me})(\text{CO})_2(\alpha\text{-diimine})]$ complexes. This is due to the weak distortion of the former complexes in their $^3\text{SBLCT}$ states as seen from the very small Stokes shifts. Remarkably, replacement of Ru by Os hardly influences the absorption and emission energies of these complexes; yet the emission lifetime is shortened because of an increase of spin-orbit coupling. The quantum yield of emission at 80 K is 1–5% for these complexes, which is lower than might be expected on the basis of their slow nonradiative decay.

Introduction

Most coordination and organometallic compounds containing a low-valent transition metal and an α -diimine ligand such as 2,2'-bipyridine (bpy) possess rather intense low-energy metal-to-ligand charge transfer (MLCT) transitions in the visible region of the spectrum. Best known are $[\text{Ru}(\text{bpy})_3]^{2+}$ ^{1,2} and $[\text{Re}(\text{Cl})(\text{CO})_3(\text{bpy})]$,^{3,4} which proved to be good photosensitizers for energy- and electron-transfer processes. Although $[\text{Ru}(\text{bpy})_3]^{2+}$ is more suitable as a photosensitizer because of its longer emission lifetime and greater stability of its oxidation product, the $[\text{Re}(\text{L})(\text{CO})_3(\alpha\text{-diimine})]^{+/0}$ complexes are more flexible because the ligand L can be varied at will,⁴ giving rise to large variation in excited-state properties. Thus, when $\text{L} = \text{Cl}^-$ is replaced by $\text{L} = \text{I}^-$, the HOMO obtains predominant halide character and the low-energy transitions change character from MLCT or $d_\pi(\text{Re}) \rightarrow \pi^*(\alpha\text{-diimine})$ to halide-to-ligand charge transfer (XLCT) or $p_\pi(\text{I}^-) \rightarrow \pi^*(\alpha\text{-diimine})$.⁵ Yet another situation arises if L is an alkyl or metal fragment bound to Re via a high-lying $\sigma(\text{Re}-\text{L})$ orbital. The lowest excited state then has $\sigma(\text{Re}-\text{L})\pi^*(\alpha\text{-diimine})$ or sigma-bond-to-ligand charge transfer (SBLCT) character.⁶ The SBLCT states are normally shorter-lived than the MLCT and XLCT states because they

give rise to homolysis of the metal-metal or metal-alkyl bond with formation of radicals. For quite a few $[\text{Re}(\text{L})(\text{CO})_3(\alpha\text{-diimine})]^{+/0}$ complexes these radicals and their formation have been studied with (time-resolved) spectroscopic techniques.^{6,7}

Interestingly, not only are most complexes photostable at low temperature but also their $^3\text{SBLCT}$ states are much longer-lived than $^3\text{MLCT}$ or $^3\text{XLCT}$ states usually are. For instance, $[\text{Re}(\text{Br})(\text{CO})_3(\text{dmb})]$ ($\text{dmb} = 4,4'$ -dimethyl-2,2'-bipyridine) emits in a 2-MeTHF glass at 80 K from its mixed $^3\text{MLCT}/^3\text{XLCT}$ state at 525 nm with a lifetime of 3.7 μs , whereas $[\text{Re}(\text{SnPh}_3)(\text{CO})_3(\text{dmb})]$ emits from its $^3\text{SBLCT}$ state at 609 nm with a lifetime of $1.1 \times 10^2 \mu\text{s}$ under these conditions.^{5,6}

To increase the variation in excited-state properties further, we have extended our photochemical studies to complexes of the type $[\text{Ru}(\text{L}_1)(\text{L}_2)(\text{CO})_2(\alpha\text{-diimine})]$, in which the two ligands L_1 and L_2 can be varied.⁸ Those complexes especially appeared to be of great interest in which both L_1 and L_2 are bound to Ru by a high-lying σ orbital. The HOMO of these complexes is a $\sigma(\text{L}_1-\text{Ru}-\text{L}_2)$ orbital, and accordingly, the SBLCT transition has $\sigma(\text{L}_1-\text{Ru}-\text{L}_2) \rightarrow \pi^*(\alpha\text{-diimine})$ character. Depending on the relative strengths of the $\text{Ru}-\text{L}_1$ and $\text{Ru}-\text{L}_2$ bonds and their involvement in the HOMO, one of these bonds is preferably broken on irradiation. If both $\text{Ru}-\text{L}_1/\text{L}_2$ bonds are strong, as in the case of $\text{L}_1 = \text{L}_2 = \text{SnPh}_3$, the complexes proved to be less

* To whom correspondence should be addressed. E-mail: stufkens@anorg.chem.uva.nl.

- (1) Meyer, T. J. *Pure Appl. Chem.* **1986**, *58*, 1193.
- (2) Juris, A.; Balzani, V.; Barigelli, F.; Campagna, S.; Belser, P.; von Zelewski, A. *Coord. Chem. Rev.* **1988**, *84*, 85.
- (3) Schanze, K. S.; MacQueen, D. B.; Perkins, T. A.; Cabana, L. A. *Coord. Chem. Rev.* **1993**, *63*.
- (4) Stufkens, D. J. *Comments Inorg. Chem.* **1992**, *13*, 359.
- (5) Rossenaar, B. D.; Stufkens, D. J.; Vlček, A., Jr. *Inorg. Chem.* **1996**, *35*, 2902.

- (6) Rossenaar, B. D.; Lindsay, E.; Stufkens, D. J.; Vlček, A., Jr. *Inorg. Chim. Acta* **1996**, *250*, 5.
- (7) Kleverlaan, C. J.; Stufkens, D. J.; Clark, I. P.; George, M. W.; Turner, J. J.; Martino, D. M.; van Willigen, H.; Vlček, A., Jr. *J. Am. Chem. Soc.* **1998**, *120*, 10871.
- (8) Aarnts, M. P.; Stufkens, D. J.; Wilms, M. P.; Baerends, E. J.; Vlček, A., Jr.; Clark, I. P.; George, M. W.; Turner, J. J. *Chem.—Eur. J.* **1996**, *2*, 1556.

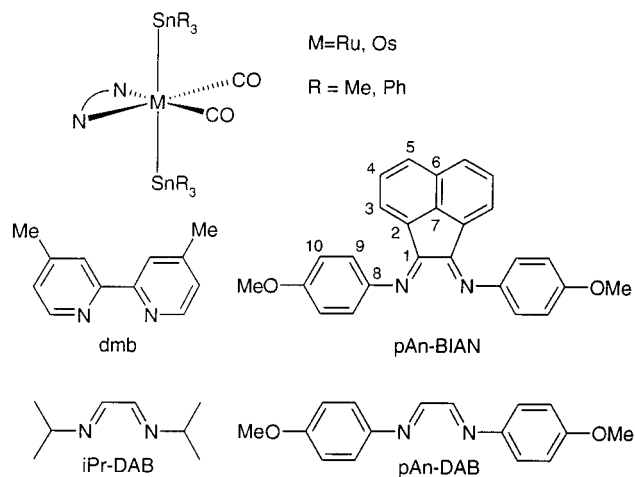


Figure 1. Schematic structures of the $[M(\text{SnR}_3)_2(\text{CO})_2(\alpha\text{-diimine})]$ complexes and the α -diimine ligands used.

photoreactive at room temperature and photostable and very long-lived in their $^3\text{SBLCT}$ state in a glass at 80 K. In the case of $[\text{Ru}(\text{SnPh}_3)_2(\text{CO})_2(\text{Pr-DAB})]$ (Pr-DAB = *N,N'*-diisopropyl-1,4-diazabutadiene) an emission lifetime of $2.6 \times 10^2 \mu\text{s}$ was measured under these conditions, which is exceptional for charge-transfer states of organometallic complexes.⁸ This result prompted us to extend our investigations of these complexes further and to develop organometallic systems that are photostable at room temperature and emit in the near-infrared region with still an appreciable lifetime to be of use as luminescent labels in biochemical separations. For this purpose, α -diimine ligands with low-lying π^* orbitals were employed in order to shift the emission to the NIR and to increase the barrier for the radical formation. To further increase the photostability, Ru was replaced by Os in $[\text{Ru}(\text{SnPh}_3)_2(\text{CO})_2(\alpha\text{-diimine})]$ because transition metal atoms from the third row are expected to form stronger bonds with tin than those of the first and second row. Figure 1 shows the general structure of the α -diimine ligands and of the complexes under study.

Experimental Section

Materials. $[\text{Ru}_3(\text{CO})_{12}]$ (ABCR), K_2OsCl_6 (Alfa), I_2 (Merck), SnClPh_3 (Merck, zur Synthese), SnClMe_3 (Acros, 99%), 4,4'-dimethyl-2,2'-bipyridine (dmb, Fluka), formic acid (Merck), and formaldehyde (aq, 40%, EGA Chemie) were used as received. Solvents purchased from Acros (THF, hexane, dichloromethane, acetonitrile, diethyl ether, methanol, 2-MeTHF), Merck (heptane), BDH (absolute ethanol), and Baker (*n*-propanol) were dried on and distilled from the appropriate drying agent when necessary. Silica gel (kieselgel 60, Merck, 70–230 mesh) for column chromatography was dried and activated by heating in vacuo at 160 °C overnight.

Syntheses. All syntheses were performed under a nitrogen atmosphere using standard Schlenk techniques. *N,N'*-Diisopropyl-1,4-diazabutadiene (Pr-DAB),⁹ *N,N'*-di(*p*-methoxyphenyl)-1,4-diazabutadiene (pAn-DAB),¹⁰ *N,N'*-bis(*p*-methoxyphenylimino)acenaphthene (pAn-BIAN),^{11,12} and $[\text{Ru}(\text{SnPh}_3)_2(\text{CO})_2(\text{Pr-DAB})]$ ¹³ were prepared according to literature procedures.

$[\text{Ru}(\text{I}_2)(\text{CO})_2(\alpha\text{-diimine})]$ (α -Diimine = pAn-DAB, pAn-BIAN, dmb). The $[\text{Ru}(\text{I}_2)(\text{CO})_2(\alpha\text{-diimine})]$ complexes were prepared accord-

ing to the procedure used for the synthesis of $[\text{Ru}(\text{I}_2)(\text{CO})_2(\text{dmb})]$. A mixture of 1.0547 g (2.14 mmol) of $[\text{Ru}(\text{I}_2)(\text{CO})_2(\text{MeCN})_2]$ and 441.6 mg (2.37 mmol) of dmb was suspended in 50 mL of diethyl ether and refluxed for 30 min. The reaction mixture was cooled to room temperature, and the residue was filtered off (G3 glass filter), washed with pentane, and dried in vacuo to yield the product as a yellow powder. Yield: 94%. IR (THF): 2049, 1991 cm^{-1} . ^1H NMR (CDCl_3): δ 2.61 (s, 6H, dmb CH_3), 7.38 (d, $^3J = 5.5$ Hz, 2H, dmb H-5), 8.22 (s, 2H, dmb H-3), 8.95 (d, $^3J = 5.8$ Hz, 2H, dmb H-6).

$[\text{Ru}(\text{I}_2)(\text{CO})_2(\text{pAn-DAB})]$: yield, ca. 90%. IR (THF): 2056, 2002 cm^{-1} . ^1H NMR (CDCl_3): δ 3.88 (s, 6H, OCH_3), 6.99 (d, $^3J = 9$ Hz, 4H, *o*- $\text{C}_6\text{H}_4\text{OCH}_3$), 7.68 (d, $^3J = 9$ Hz, 4H, *m*- $\text{C}_6\text{H}_4\text{OCH}_3$), 8.12 (s, 2H, imine H).

$[\text{Ru}(\text{I}_2)(\text{CO})_2(\text{pAn-BIAN})]$: yield, ca. 90%. IR (THF): 2056, 2003 cm^{-1} . ^1H NMR (CDCl_3): δ 3.95 (s, 6H, OCH_3), 7.12 (d, $^3J = 9$ Hz, 6H, H3 + H9; see Figure 1 for numbering), 7.52 (pst, 2H, H4), 7.80 (d, $^3J = 8.8$ Hz, 4H, H10), 8.04 (d, 2H, $^3J = 8.3$ Hz, H5).

$[\text{Os}(\text{Cl})_2(\text{CO})_2]_n$. The polymer $[\text{Os}(\text{Cl})_2(\text{CO})_2]_n$ was prepared according to modified literature procedure.¹⁴ K_2OsCl_6 (823.3 mg, 1.7 mmol) was dissolved in a mixture of formic acid (40 mL) and formaldehyde (aq, 40%, 15 mL). The reaction mixture was deaerated by bubbling nitrogen through for 20 min and subsequently refluxed for 3 days during which the color changed from dark-red to greenish to light-yellow. The solvent was removed in vacuo, and the resulting product was triturated with dichloromethane. The product was dissolved in acetone and filtered to remove KCl. Evaporation of the solvent yielded the product as an off-white powder. Yield: ca. 90%. IR (THF): 2117, 2022 cm^{-1} .

$[\text{Os}(\text{Cl})_2(\text{CO})_2(\text{dmb})]$. $[\text{Os}(\text{Cl})_2(\text{CO})_2(\text{dmb})]$ was prepared according to a modified literature procedure.¹⁴ $[\text{Os}(\text{Cl})_2(\text{CO})_2]_n$ (269.0 mg, 0.85 mmol) and dmb (180.2 mg, 0.97 mmol) were dissolved in 30 mL of *n*-propanol. The reaction mixture was refluxed for several hours until IR spectral results showed complete conversion. After the solvent was removed in vacuo, the product was purified by column chromatography (activated silica, hexane/dichloromethane gradient elution). The product was obtained as a light-yellow powder. Yield: ca. 90%. IR (THF): 2030, 1960 cm^{-1} . UV-vis (THF), λ_{max} : 296, 373 nm. ^1H NMR (CDCl_3): δ 2.63 (s, 6H, dmb CH_3), 7.45 (d, $^3J = 5.3$ Hz, 2H, dmb H-5), 8.02 (s, 2H, dmb H-3), 8.94 (d, $^3J = 5.7$ Hz, 2H, dmb H-6).

$[\text{Os}(\text{Cl})_2(\text{CO})_2(\text{Pr-DAB})]$. $[\text{Os}(\text{Cl})_2(\text{CO})_2]_n$ (201.1 mg, 0.63 mmol) and Pr-DAB (182.1 mg, 1.30 mmol) were dissolved in 30 mL of absolute ethanol. The reaction mixture was refluxed for several hours until IR results showed complete conversion. The solvent was evaporated, and after purification by column chromatography (activated silica, hexane/THF = 1:1), the product was obtained as an orange powder. Yield: 63%. IR (THF): 2034, 1965 cm^{-1} . UV-vis (THF), λ_{max} : 419 nm. ^1H NMR (CDCl_3): δ 1.50, 1.52 (d, $^3J = 6.6$ Hz, 12H, $\text{CH}(\text{CH}_3)_2$), 4.32 (sept, $^3J = 6.5$ Hz, 2H, $\text{CH}(\text{CH}_3)_2$), 8.55 (s, 2H, imine-CH).

$[\text{Ru}(\text{SnPh}_3)_2(\text{CO})_2(\text{dmb})]$. $[\text{Ru}(\text{I}_2)(\text{CO})_2(\text{dmb})]$ (206.2 mg, 0.35 mmol) was dissolved in 25 mL of THF. A solution of LiSnPh_3 in THF (prepared from SnClPh_3 and freshly cut lithium metal) was added gradually (in the dark) until IR results showed complete conversion. Methanol (2 mL) was added to quench any unreacted LiSnPh_3 . The solvent was evaporated, and after purification by column chromatography in the dark (activated silica, hexane/dichloromethane gradient elution) the product was obtained as a red microcrystalline powder. Yield: ca. 50%. Anal. Calcd for $\text{C}_{50}\text{H}_{42}\text{N}_2\text{O}_2\text{RuSn}_2$: C, 57.67; H, 4.07; N, 2.69. Found: C, 57.33; H, 3.91; N, 2.58. FAB-MS m/z : 1042 (M^+), 965 [$\text{M}^+ - \text{Ph}$], 691 [$\text{M}^+ - \text{SnPh}_3$]. IR (THF): 1996, 1942 cm^{-1} . UV-vis (THF), λ_{max} : 327, 521 nm. ^1H NMR (C_6D_6): δ 1.65 (s, $J_{\text{Sn-H}} = 9$ Hz, 6H, dmb CH_3), 5.80 (d, $^3J = 5.6$ Hz, 2H, dmb H5), 6.66 (s, dmb H3), 7.02 (m, 9H, *m/p*- SnC_6H_5), 7.41 (m, 6H, *o*- SnC_6H_5), 8.29 (d, $^3J = 5.9$ Hz, 2H, dmb H-6). ^{13}C NMR (C_6D_6): δ 20.2 (dmb-Me), 122.8 (dmb C-5), 125.4 (dmb C-3), 127.1 (*p*- SnC_6H_5), 127.7 (*m*- SnC_6H_5), 137.4 ($J_{\text{Sn-C}} = 36$ Hz, *o*- SnC_6H_5), 145.1 (dmb C-4), 145.4 (dmb C-2), 150.7 ($J_{\text{Sn-C}} = 12$ Hz, *ipso*- SnC_6H_5), 151.8 ($J_{\text{Sn-C}} = 12$ Hz, dmb C-6), 208.0 (CO).

(9) Kliegman, J. M.; Barnes, R. K. *Tetrahedron* **1970**, *26*.
 (10) Kliegman, J. M.; Barnes, R. K. *J. Org. Chem.* **1970**, *35*, 3140.
 (11) Van Asselt, R.; Gielens, E. E. C. G.; Rülke, R. E.; Vrieze, K.; Elsevier, C. J. *J. Am. Chem. Soc.* **1994**, *116*, 977.
 (12) Van Asselt, R.; Elsevier, C. J.; Smeets, W. J. J.; Spek, A. L.; Benedix, R. *Recl. Trav. Chim. Pays-Bas* **1994**, *113*, 88.
 (13) Aarnts, M. P.; Stufkens, D. J.; Oskam, A.; Fraanje, J.; Goubitz, K. *Inorg. Chim. Acta* **1997**, *256*, 93.

(14) Jandrasics, E. Z.; Keene, F. R. *J. Chem. Soc., Dalton Trans.* **1997**, 153.

[Ru(SnPh₃)₂(CO)₂(pAn-DAB)]. To a solution of 285 mg of [Ru(I)₂(CO)₂(pAn-DAB)] in THF, 0.5 mL of NaK₃ alloy was added. Stirring at room temperature yielded a solution of a highly reactive anionic intermediate. The remaining NaK₃ alloy was filtered off using a G3 frit, and 2 equiv of SnClPh₃ were added in the dark. After column chromatography (activated silica, dichloromethane/hexane gradient elution) the product was obtained as a brownish-green powder. Yield: ca. 50%. FAB-MS *m/z*: 1126 (M⁺), 1049 (M⁺ - Ph), 776 (M⁺ - SnPh₃). IR (THF): 2011, 1960 cm⁻¹. UV-vis (THF), λ_{max}: 396, 449, 570 nm. ¹H NMR (C₆D₆): δ 3.18 (s, 6H, OCH₃), 6.63 (d, ³J = 9 Hz, 4H, *o*-C₆H₄OCH₃), 6.82 (s, J_{Sn-H} = 27 Hz, 2H, imine H), 7.09 (d, ³J = 9 Hz, 4H, *m*-C₆H₄OCH₃), 7.19 (m, 18H, *m/p*-SnC₆H₅), 7.50 (m, 12H, *o*-SnC₆H₅). ¹³C NMR APT (C₆D₆): δ 55.1 (OCH₃), 114.4 (*o*-C₆H₄OCH₃), 124.5 (*m*-C₆H₄OCH₃), 127.1 (*p*-C₆H₄OCH₃), 128 (*m/p*-SnC₆H₅), 138.0 (J_{Sn-C} = 35 Hz, *o*-SnC₆H₅), 141.3 (*ipso*-SnC₆H₅), 160.5 (s, J_{Sn-C} = 15 Hz, imine C), 204.0 (CO).

[Ru(SnPh₃)₂(CO)₂(pAn-BIAN)]. This complex was prepared from [Ru(I)₂(CO)₂(pAn-BIAN)] and SnClPh₃ according to the procedure for [Ru(SnPh₃)₂(CO)₂(pAn-DAB)]. Yield: ca. 50%. FAB-MS *m/z*: 1250 (M⁺), 1173 (M⁺ - Ph), 899 (M⁺ - SnPh₃). IR (THF): 2011, 1960 cm⁻¹. UV-vis (THF), λ_{max}: 272, 321, 377sh, 400sh, 455, 607 nm. ¹H NMR (CD₂Cl₂): δ 3.86 (s, 6H, OCH₃), 6.63 (d, ³J = 8.7 Hz, 4H, H10; see Figure 1 for numbering), 6.73 (d, ³J = 7.2 Hz, 2H, H3), 6.9 (m, 18H, *m/p*-SnC₆H₅), 7.03 (d, ³J = 8.7 Hz, 4H, H9), 7.24 (m, 12H, *o*-Sn-C₆H₅), 7.28 (pst, 2H, H4), 7.82 (d, 2H ³J = 8.4 Hz, H5). ¹³C NMR APT (CD₂Cl₂): δ 56.2 (OCH₃), 114.1 (C9; see Figure 1 for numbering), 122.8 (C3) 124.6 (C10), 127.7 (C4), 128.1 (*p*-SnC₆H₅), 128.4 (*m*-SnC₆H₅), 128.5 (C2), 128.7 (C5), 131.1 (C6), 138.0 (J_{Sn-C} = 34 Hz, *o*-SnC₆H₅), 140.7 (C7), 142.9 (*ipso*-SnC₆H₅), 144.3 (C8), 159.9 (C11), 161.6 (C1), 204.08 (CO).

[Ru(SnMe₃)₂(CO)₂(α-diimine)] (α-diimine = dmb, ¹Pr-DAB). The [Ru(SnMe₃)₂(CO)₂(α-diimine)] complexes were prepared by reaction of [Ru(I)₂(CO)₂(α-diimine)] and LiSnMe₃ according to the procedure used for the synthesis of [Ru(SnPh₃)₂(CO)₂(dmb)] (vide supra).

[Ru(SnMe₃)₂(CO)₂(¹Pr-DAB)]: yield, ca. 50%. IR (THF): 1993, 1936 cm⁻¹. UV-vis (THF), λ_{max}: 277, 404, 511 nm. ¹H NMR (CDCl₃): δ 0.03 (s, J_{Sn-H} = 43 Hz, 18H, SnMe), 1.38 (d, 12H, ³J = 6.6 Hz, CH(CH₃)₂), 4.47 (septet, 2H, ³J = 6.6 Hz, CH(CH₃)₂), 7.82 (s, J_{Sn-H} = 26 Hz, 2H, imine H). ¹³C NMR APT (C₆D₆): δ -8.5 (J_{Sn-C} = 198 Hz, SnCH₃), 25.0 (CH(CH₃)₂), 63.8 (CH(CH₃)₂), 141.6 (imine-C), 181.5 (J_{Sn-C} = 48 Hz, CO).

[Ru(SnMe₃)₂(CO)₂(dmb)]: yield, ca. 50%. IR (THF): 1984, 1928 cm⁻¹. UV-vis (THF), λ_{max}: 257sh, 409, 598 nm. ¹H NMR (C₆D₆): δ 0.10 (s, J_{Sn-H} = 38 Hz, 18H, SnMe 2.63 (s, J_{Sn-H} = 11 Hz, 6H, dmb CH₃), 6.07 (d, ³J = 5.9 Hz, 2H, dmb H-5), 7.08 (s, 2H, dmb H3), 8.70 (d, ³J = 5.9 Hz, 2H, dmb H6). ¹³C NMR APT (C₆D₆): δ -10.1 (SnMe), 20.5 (dmb CH₃), 122.8 (J_{Sn-C} = 13 Hz, dmb C5), 124.4 (J_{Sn-C} = 8 Hz, dmb C3), 144.3 (J_{Sn-C} = 16 Hz, dmb C4), 149.7 (J_{Sn-C} = 16 Hz, dmb C2), 151.5 (J_{Sn-C} = 12 Hz, dmb C6), 210.5 (CO).

[Os(SnPh₃)₂(CO)₂(dmb)]. [Os(Cl)₂(CO)₂(dmb)] (332.4 mg, 0.66 mmol) was dissolved in 25 mL of THF. A solution of LiSnPh₃ in THF (prepared from SnClPh₃ and freshly cut lithium metal) was added gradually (in the dark) until IR results showed complete conversion. Methanol (2 mL) was added to quench any unreacted LiSnPh₃. The solvent was evaporated, and after purification by column chromatography in the dark (silica, hexane/dichloromethane gradient elution) the product was obtained as a red microcrystalline powder. Yield: ca. 50%. FAB-MS *m/z*: 1130 (M⁺), 1053 [M⁺ - Ph], 781 [M⁺ - SnPh₃]. IR (THF): 1989, 1930 cm⁻¹. UV-vis (THF), λ_{max}: 305, 358sh, 514 nm. ¹H NMR (C₆D₆): δ 1.67 (s, J_{Sn-H} = 9 Hz, 6H, dmb CH₃), 5.71 (d, ³J = 5.9 Hz, 2H, dmb H5), 6.62 (s, dmb H3), 7.02 (m, 9H, *m/p*-SnC₆H₅), 7.41 (m, 6H, *o*-SnC₆H₅), 8.45 (d, ³J = 6.0 Hz, 2H, dmb H6), ¹³C NMR APT (C₆D₆): δ 20.1 (dmb CH₃), 123.1 (dmb C5), 126.2 (dmb C3), 127.2 (*m/p*-SnC₆H₅), 127.7 (*m/p*-SnC₆H₅), 137.5 (J_{Sn-C} = 35 Hz, *o*-SnC₆H₅), 144.0 (J_{Sn-C} = 16 Hz, dmb C4), 145.2 (J_{Sn-C} = 13 Hz, dmb C2), 151.7 (dmb C6), 150.7 (J_{Sn-C} = 11 Hz, *ipso*-SnC₆H₅), 190.8 (CO).

[Os(SnPh₃)₂(CO)₂(¹Pr-DAB)]. Os(Cl)₂(CO)₂(¹Pr-DAB) (182.5 mg, 0.40 mmol) was dissolved in 30 mL of THF. After addition of NaK_{2.8} alloy (0.5 mL), the color changed from orange to green to brown-yellow. The reaction mixture was filtered and added in the dark to a solution

of 292.8 mg (0.88 mmol) of SnClPh₃ in 10 mL of THF. This mixture was stirred for a few minutes, and the solvent was removed in vacuo. After purification by column chromatography in the dark (silica, hexane/dichloromethane gradient elution) the product was obtained as an orange microcrystalline powder. Yield: ca. 50%. FAB-MS *m/z*: 1086 [M⁺], 1009 [M⁺ - Ph], 737 [M⁺ - SnPh₃]. IR (THF): 1996, 1939 cm⁻¹. UV-vis (THF), λ_{max}: 287, 494 nm. ¹H NMR (CDCl₃): δ 0.95 (d, ³J = 6.6 Hz, 12H, CH(CH₃)₂), 4.62 (sept, ³J = 6.6 Hz, 2H, CH(CH₃)₂), 7.25 (m, 9H, *m/p*-SnC₆H₅), 7.32 (m, 6H, *o*-SnC₆H₅), 8.15 (s, J_{Sn-H} = 23.7 Hz, 2H, imine H). ¹³C NMR APT (C₆D₆): δ 24.8 (CH(CH₃)₂), 65.4 (CH(CH₃)₂), 128.0 (*m/p*-SnC₆H₅), 128.2 (*m/p*-SnC₆H₅), 137.7 (J_{Sn-C} = 34 Hz, *o*-SnC₆H₅), 142.7 (*ipso*-SnC₆H₅), 148.5 (J_{Sn-C} = 15 Hz, imine C), 187.9 (CO).

[Os(SnMe₃)₂(CO)₂(¹Pr-DAB)]. [Os(SnMe₃)₂(CO)₂(¹Pr-DAB)] was prepared from [Os(Cl)₂(CO)₂(¹Pr-DAB)] and LiSnMe₃ according to the procedure used for the synthesis of [Ru(SnPh₃)₂(CO)₂(dmb)] (vide supra). Yield: ca. 50%. IR (THF): 1984, 1927 cm⁻¹. UV-vis (THF), λ_{max}: 257, 370, 484 nm. ¹H NMR (C₆D₆): δ 0.28 (s, 18H, J_{Sn-H} = 46 Hz, SnMe), 1.04 (d, 12H, ³J = 6.6 Hz, CH(CH₃)₂), 4.47 (septet, 2H, ³J = 6.6 Hz, CH(CH₃)₂), 7.52 (s, J_{Sn-H} = 22 Hz, 2H, imine H). ¹³C NMR APT (C₆D₆): δ -9.7 (J_{Sn-C} = 228 Hz, SnCH₃), 25.2 (CH(CH₃)₂), 65.0 (CH(CH₃)₂), 143.0 (imine-C), 190.9 (J_{Sn-C} = 38 Hz, CO).

Spectroscopic Measurements. All spectroscopic measurements were performed under a nitrogen atmosphere. Infrared spectra were recorded on Bio-Rad FTS-7 and FTS-60A FTIR spectrophotometers (the latter equipped with a liquid-nitrogen-cooled MCT detector) and electronic absorption spectra on Varian Cary 4E and Hewlett-Packard 8453 spectrophotometers. NMR spectra were recorded on a Bruker AMX 300 (300.13 and 75.46 MHz for ¹H and ¹³C, respectively) spectrometer. Resonance Raman spectra of the complexes dispersed in KNO₃ pellets were recorded on a Dilor XY spectrometer equipped with a Wright Instruments CCD detector, using a Spectra Physics 2040E Ar⁺ and Coherent CR490 and CR590 dye lasers (with Coumarin 6 and Rhodamine 6G dyes) as excitation sources. Steady-state emission spectra were measured on a SPEX Fluorolog 2 (equipped with an RCA C31034 Peltier cooled GaAs photomultiplier).

Nanosecond time-resolved electronic absorption and emission spectra were obtained using a setup described previously.⁷ A Teflon mask around the glass tube sample cell with 1 mm holes for the probe light and a 1 cm slit for the pump light was used for the low-temperature transient absorption spectrum. As irradiation sources, the second harmonic (532 nm) of a Spectra Physics GCR3 Nd:YAG laser, a Quanta Ray PDL pulsed dye laser with a Coumarin 440 solution (440 nm), or a continuously tunable (360–700 nm) Coherent Infinity XPO laser were used. Emission quantum yields were measured relative to a standard solution of [Re(Cl)(CO)₃(bpy)] in 2-MeTHF (Φ = 0.028 at 77 K), using a gate of 10 ms.

Photochemical quantum yields were determined by observation of the decay of the first absorption band of solutions of the complexes in dichloromethane at 21.0 °C by in situ irradiation in a Varian Cary 4E spectrophotometer using previously described procedures.⁷

Results

(I) Syntheses. The procedure used for the synthesis of [Ru(SnPh₃)₂(CO)₂(¹Pr-DAB)]¹⁵ is not suitable for the preparation of the [Ru(SnR₃)₂(CO)₂(α-diimine)] complexes containing α-diimine ligands other than R-DAB. Instead, these complexes were prepared from [Ru(I)₂(CO)₂(α-diimine)], which was obtained by reaction of the appropriate α-diimine ligand with [Ru(I)₂(CO)₂(MeCN)₂]¹⁶ and LiSnR₃.

However, during the preparation of [Ru(SnPh₃)₂(CO)₂(pAn-BIAN)] the last step resulted in decomposition. [Ru(I)₂(CO)₂(pAn-BIAN)] was therefore prepared first and subsequently reduced using a sodium-potassium alloy to give a highly

(15) Aarnts, M. P.; Wilms, M. P.; Peelen, K.; Fraanje, J.; Goubitz, K.; Hartl, F.; Stufkens, D. J.; Baerends, E. J.; Vlček, A., Jr. *Inorg. Chem.* **1996**, *35*, 5468.

(16) Irving, R. J. *J. Chem. Soc.* **1956**, 2879.

Table 1. Electronic Absorption Spectral Data and Transient Absorption Lifetimes of the $M(\text{SnR}_3)_2(\text{CO})_2(\alpha\text{-diimine})$ Complexes at Room Temperature

entry	metal	R	α -diimine	electronic absorption (nm)			Δ^b (nm)	transient lifetime ^c (μs)
				toluene	CH_2Cl_2 (ϵ) ^a	MeCN		
1 ^d	Ru	Ph	ⁱ Pr-DAB	523	519 (6.8)	508	0.57	1.0
2	Ru	Ph	pAn-DAB	577	572 (2.7)	567	0.31	1.9
3	Ru	Ph	pAn-BIAN	614	605 (16)	601	0.35	3.6
4	Ru	Ph	dmb	542	529 (3.8)	503	1.4	1.0
5	Ru	Me	ⁱ Pr-DAB	517	515 (7.2)	511	0.23	2.6 ^e
6	Ru	Me	dmb	630	612 (5.3)	581	1.3	0.50
7	Os	Ph	ⁱ Pr-DAB	497	495 (6.2)	485	0.50	1.5
8	Os	Ph	dmb	537	519 (4.1)	496	1.5	2.5
9	Os	Me	ⁱ Pr-DAB	485	484 (6.9)	482	0.13	1.4

^a ϵ in $10^3 \text{ M}^{-1} \text{ cm}^{-1}$. ^b $\Delta = \nu_{\text{max}}(\text{MeCN}) - \nu_{\text{max}}(\text{toluene})$ in 10^3 cm^{-1} . ^c In THF at room temperature. ^d From ref 13. ^e Uncertainty is large because of overlap of transient and ground-state absorptions.

Table 2. Resonance Raman Data of the Complexes $[\text{M}(\text{SnR}_3)_2(\text{CO})_2(\text{Pr-DAB})]$ ($\text{M} = \text{Ru, Os}$; $\text{R} = \text{Ph, Me}$) and $[\text{Ru}(\text{Cl})(\text{Me})(\text{CO})_2(\text{Pr-DAB})]$ in KNO_3

metal	R	resonance Raman data									
		$\nu_s(\text{CO})$	$\nu_s(\text{CN})$	$\delta_s(\text{CH})$	$\delta(\text{DAB})$						
Ru ^a	Ph	1473s	1283s	1166w	953s	836s	651w	610m	419w	247m	197m
Os	Ph	1467s	1272s	1168w	958s	844s	657w	614m	424m	256m	211w
Ru	Me	1473s	1286s	1178s	971s	850s	651m	615m	496w	425w	264w
Os	Me	1470m	1279s	1172s	968s	850s	646w	614m	494w	420m	251w
RuClMe ^b		2033w	1568s						487m		

^a From ref 8. ^b $[\text{Ru}(\text{Cl})(\text{Me})(\text{CO})_2(\text{Pr-DAB})]$, from ref 17.

reactive intermediate. This intermediate was then allowed to react with 2 equiv of SnClPh_3 , yielding the desired product. This method, which has also been used for the synthesis of $[\text{Ru}(\text{Me})(\text{I})(\text{CO})_2(\text{bpy})]$,^{17,18} was also successfully used for the synthesis of $[\text{Ru}(\text{SnPh}_3)_2(\text{CO})_2(\text{pAn-DAB})]$.

The recently synthesized complexes $[\text{Os}(\text{Cl})_2(\text{CO})_2(\alpha\text{-diimine})]$ ¹⁴ proved to be excellent starting compounds for the preparation of $[\text{Os}(\text{SnPh}_3)_2(\text{CO})_2(\alpha\text{-diimine})]$. The synthesis started with the formation of the polymer $[\text{Os}(\text{Cl})_2(\text{CO})_2]_n$, which was allowed to react with the α -diimine ligand. Subsequent addition of LiSnPh_3 to a solution of this complex afforded $[\text{Os}(\text{SnPh}_3)_2(\text{CO})_2(\alpha\text{-diimine})]$ in the case of dmb. However, in the case of the ⁱPr-DAB complex, the last step of this reaction sequence resulted in decomposition, and $[\text{Os}(\text{SnPh}_3)_2(\text{CO})_2(\text{Pr-DAB})]$ was therefore synthesized from $[\text{Os}(\text{Cl})_2(\text{CO})_2(\text{Pr-DAB})]$ using the procedure used for $[\text{Ru}(\text{SnPh}_3)_2(\text{CO})_2(\text{pAn-BIAN})]$.

All compounds are strongly colored microcrystalline powders. They have a *trans*-(SnR_3 , SnR_3), *cis*-(CO , CO) configuration, as can be seen from their IR and NMR spectra.¹³ The complexes are photostable in the solid state but photolabile in solution to varying degrees.

(II) Electronic Absorption and Resonance Raman Spectra.

All complexes under study show an intense absorption band at 500–600 nm (Table 1), which has been assigned to a $\sigma(\text{Sn}-\text{Ru}-\text{Sn}) \rightarrow \pi^*(\text{Pr-DAB})$ sigma-bond-to-ligand charge transfer transition in the case of $[\text{Ru}(\text{SnPh}_3)_2(\text{CO})_2(\text{Pr-DAB})]$.¹³ The absorption bands are only weakly solvatochromic. For instance, $\Delta\nu = \nu_{\text{max}}(\text{MeCN}) - \nu_{\text{max}}(\text{toluene}) = 0.57 \times 10^3 \text{ cm}^{-1}$ for $[\text{Ru}(\text{SnPh}_3)_2(\text{CO})_2(\text{Pr-DAB})]$, which is much less than the solvatochromism of the MLCT band of, for example, the isostructural complex $[\text{Ru}(\text{Cl})(\text{Me})(\text{CO})_2(\text{Pr-DAB})]$ ($\Delta\nu = 1.9 \times 10^3 \text{ cm}^{-1}$).¹⁷ Furthermore, the absorption bands of the R-DAB and pAn-BIAN complexes (Table 1, entries 1, 2, 5, 7, and 9) are

less solvatochromic ($\Delta\nu = 0.2 \times 10^3$ to $0.6 \times 10^3 \text{ cm}^{-1}$) than those of the aromatic dmb complexes ($\Delta\nu = 1.2 \times 10^3$ to $1.5 \times 10^3 \text{ cm}^{-1}$) (Table 1, entries 4, 6, and 8).

On going to a 2-MeTHF glass at 80 K, the absorption bands of the complexes become narrower and shift by ca. 20 nm to shorter wavelengths. They become asymmetric for the R-DAB complexes, while those of the aromatic α -diimine compounds show a pronounced shoulder on their short-wavelength side. Because the DFT calculations on the model complex $[\text{Ru}(\text{SnH}_3)_2(\text{CO})_2(\text{H-DAB})]$ do not show the presence of any close-lying electronic transition,¹⁵ this shoulder is attributed to a vibrational sideband.

To further characterize the SBLCT transition, we studied the resonance Raman (rR) spectra of the complexes. Upon excitation into an allowed electronic transition, such rR spectra normally show resonance enhancement of Raman intensity for those vibrations that are most strongly coupled to this transition.¹⁹ In other words, this technique allows us to characterize the electronic transition by revealing which bonds of the complex are affected most. RR spectra were recorded for all $[\text{M}(\text{SnR}_3)_2(\text{CO})_2(\text{Pr-DAB})]$ ($\text{M} = \text{Ru, Os}$; $\text{R} = \text{Me, Ph}$) complexes under study and for comparison also for $[\text{Ru}(\text{Cl})(\text{Me})(\text{CO})_2(\text{Pr-DAB})]$ in order to find out in which way the rR spectra are affected by the type of electronic transition (SBLCT vs MLCT). The wavenumbers of the most strongly enhanced Raman bands are collected in Table 2. The spectrum of $[\text{Ru}(\text{Cl})(\text{Me})(\text{CO})_2(\text{Pr-DAB})]$ is rather simple (Figure 2a); it shows a strong rR effect for $\nu_s(\text{CN})$ of the ⁱPr-DAB ligand at 1568 cm^{-1} and for a band at 487 cm^{-1} , belonging to either $\nu(\text{Ru}-\text{CH}_3)$ or $\nu_s(\text{Ru}-\text{CO})$. A weaker effect is observed for $\nu_s(\text{CO})$ at 2033 cm^{-1} . This spectrum is characteristic of excitation into an MLCT transition because such a transition is accompanied by reduction of the ⁱPr-DAB ligand (rR effect for $\nu_s(\text{CN})$) and oxidation of the central metal atom (rR effect for $\nu_s(\text{CO})$).

(17) Nieuwenhuis, H. A.; Stufkens, D. J.; Oskam, A. *Inorg. Chem.* **1994**, *33*, 3212.

(18) Rohde, W.; tom Dieck, H. *J. Organomet. Chem.* **1987**, *328*, 209.

(19) Clark, R. J. H.; Dines, T. J. *Angew. Chem., Int. Ed. Engl.* **1986**, *25*, 131.

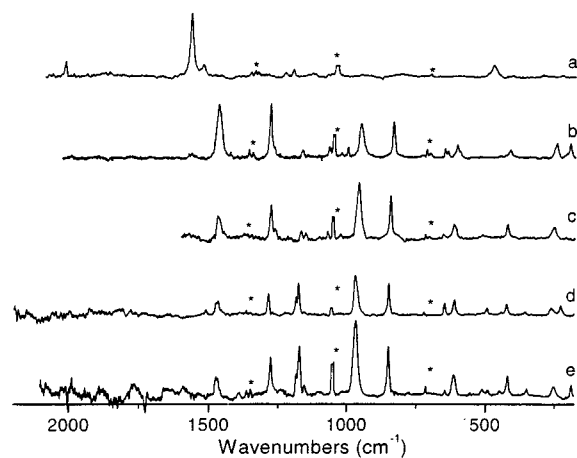


Figure 2. Resonance Raman spectra of (a) [Ru(Cl)(Me)(CO)₂(ⁱPr-DAB)] ($\lambda_{\text{exc}} = 457.9$ nm), (b) [Ru(SnPh₃)₂(CO)₂(ⁱPr-DAB)] ($\lambda_{\text{exc}} = 457.9$ nm), (c) [Os(SnPh₃)₂(CO)₂(ⁱPr-DAB)] ($\lambda_{\text{exc}} = 488.0$ nm), (d) [Ru(SnMe₃)₂(CO)₂(ⁱPr-DAB)] ($\lambda_{\text{exc}} = 476.5$ nm), and (e) [Os(SnMe₃)₂(CO)₂(ⁱPr-DAB)] ($\lambda_{\text{exc}} = 476.5$ nm). Asterisks denote NO₃⁻ peaks.

The bands observed in the rR spectra of the [M(SnPh₃)₂(CO)₂(ⁱPr-DAB)] complexes are weaker than those of [Ru(Cl)(Me)(CO)₂(ⁱPr-DAB)], while more bands are resonantly enhanced. The spectra of, for example, [Ru(SnPh₃)₂(CO)₂(ⁱPr-DAB)] show rR effects for stretching and deformation modes of the ⁱPr-DAB ligand (1473, 1283, 953, and 836 cm⁻¹), while $\nu_s(\text{CO})$ is not observed at all. Some of these resonance effects are exceptional, and their occurrence will be explained in the Discussion. In addition, several lower-frequency rR bands (at 610, 419, 247, and 197 cm⁻¹ for [Ru(SnPh₃)₂(CO)₂(ⁱPr-DAB)]) are observed, which belong to (combined) metal–ligand stretching and deformation modes.^{20,21} The band at about 250 cm⁻¹ is tentatively assigned to a vibration having predominant $\nu(\text{M}-\text{Sn})$ or $\nu(\text{Sn}-\text{M}-\text{Sn})$ (M = Ru, Os) character because it is observed for all SnR₃ complexes having a lowest SBLCT transition, but not for any other complex. The corresponding osmium complex [Os(SnPh₃)₂(CO)₂(ⁱPr-DAB)] has virtually the same rR spectrum, while the spectra of the corresponding [M(SnMe₃)₂(CO)₂(ⁱPr-DAB)] complexes additionally show a strong rR effect for a band at ca. 1170 cm⁻¹, which is assigned to a CH₃ deformation mode of the SnMe₃ ligand.²²

(III) Time-Resolved Electronic Absorption and Emission Spectra. Nanosecond time-resolved absorption (TA) spectra of the complexes were measured in THF at room temperature and for [Os(SnPh₃)₂(CO)₂(dmb)] also in a 2-MeTHF glass at 90 K. Both spectra of the latter complex are shown in Figure 3. In most spectra the bleaching of the ground-state absorption is not observed because of the much stronger excited-state absorption. The TA spectra of all complexes are very similar and consist of strong absorptions with maxima at ca. 350 and 530 nm and a weak, broad band above 600 nm. The low-temperature spectrum of [Os(SnPh₃)₂(CO)₂(dmb)] shows that this latter absorption is a separate band and not the tail of the 530 nm band. The 90 K spectrum of [Os(SnPh₃)₂(CO)₂(dmb)] shows that the 530 nm absorption band consists of two components. Similar features, i.e., a broad, composite band around 500 nm, a very broad and weak absorption above 600 nm, and an intense

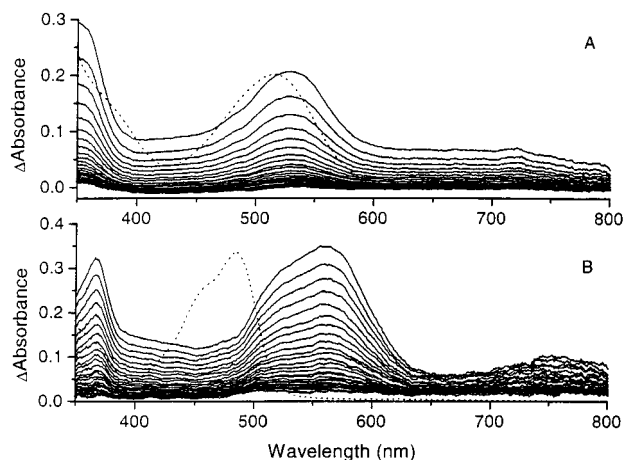


Figure 3. Transient absorption difference spectra (solid lines) and ground-state absorption spectra (dotted lines) of [Os(SnPh₃)₂(CO)₂(dmb)] in THF at room temperature (A) and in a 2-MeTHF glass at 90 K (B). The delays between the transient absorption spectra are 200 ns (A) and 20 μs (B).

band between 350 and 400 nm, have also been observed in the TA spectra of [Re(Br)(CO)₃(dmb)],²³ [Re(SnPh₃)(CO)₃(dmb)],⁶ and [Re(CH₃)(CO)₃(dmb)]⁷ and in the spectrum of reduced [Re(Br)(CO)₃(dmb)].²³ They closely resemble the bands found in the absorption spectrum of the [dmb]⁻ radical anion²⁴ and are therefore assigned to the intraligand transitions of the [dmb]⁻ radical anion in the SBLCT states of the complexes. At room temperature the excited states, which have lifetimes varying between 0.5 and 3.6 μs , are quenched by oxygen, which confirms their triplet character. For instance, the transient lifetime of [Os(SnPh₃)₂(CO)₂(dmb)] is reduced by a factor of 10 in the presence of oxygen.

Nanosecond time-resolved emission spectra were recorded for the compounds in a 2-MeTHF glass at 90 K, under which conditions the complexes are completely photostable. The emission data, collected in Table 3, show that the emitting states of all [M(SnR₃)₂(CO)₂(α-diimine)] complexes are very long-lived, much longer than the ³MLCT state of the structurally related compound [Ru(Cl)(Me)(CO)₂(ⁱPr-DAB)]. The longest lifetime ($\tau = 1.1$ ms) is observed for [Ru(SnPh₃)₂(CO)₂(dmb)], in which complex the dmb is a rigid aromatic ligand. The SnMe₃-substituted complexes have slightly shorter emission lifetimes than the SnPh₃ ones, which were previously observed for [Re(SnR₃)(CO)₃(phen)] (R = Me, Ph).²⁵

Figure 4 shows the absorption and excitation spectra of [Ru(SnPh₃)₂(CO)₂(dmb)], together with its continuous wave emission spectrum excited at 500 nm. The excitation spectrum does not deviate from the absorption spectrum, which means that the population of the emissive state has the same efficiency throughout the first absorption band.

Just as for [Ru(SnPh₃)₂(CO)₂(ⁱPr-DAB)]⁸ a weak emission is observed at the low-energy side of the broad emission band, which is only produced by excitation at the low-energy side of the first absorption band. Its lifetime is somewhat shorter than that of the much stronger high-energy component. For instance, the emission of [Ru(SnPh₃)₂(CO)₂(dmb)] has a lifetime of 1.1 ms at 440 nm excitation (Table 3) and 0.76 ms at 532 nm excitation. Because the lifetimes do not differ much, taking into

(20) Kokkes, M. W.; Snoeck, T. L.; Stufkens, D. J.; Oskam, A.; Christophersen, M.; Stam, C. H. *J. Mol. Struct.* **1985**, *131*, 11.

(21) Andréa, R. R.; de Lange, W. G. J.; Stufkens, D. J.; Oskam, A. *Inorg. Chim. Acta* **1988**, *149*, 77.

(22) Kleverlaan, C. J.; Stufkens, D. J.; Fraanje, J.; Goubitz, K. *Eur. J. Inorg. Chem.* **1998**, 1243.

(23) Rossenaar, B. D.; Stufkens, D. J.; Vlček, A., Jr. *Inorg. Chim. Acta* **1996**, *247*, 247.

(24) Krejčík, M.; Vlček, A. A. *J. Electroanal. Chem.* **1991**, *313*, 243.

(25) Luong, J. C.; Faltynek, R. A.; Wrighton, M. S. *J. Am. Chem. Soc.* **1980**, *102*, 7892.

Table 3. Emission Data of $[M(\text{SnR}_3)_2(\text{CO})_2(\alpha\text{-diimine})]$ and $[\text{Ru}(\text{Cl})(\text{Me})(\text{CO})_2(^i\text{Pr-DAB})]$ in a 2-MeTHF Glass at 90 K

entry	metal	R	α -diimine	λ_{abs} (nm)	λ_{em} (nm)	$\Delta E_{\text{abs-em}}$ (10^3 cm^{-1})	τ ($10^2 \mu\text{s}$)	Φ_{em} (10^{-2})	$\Phi_{\text{ISC}k_r}$ (10^2 s^{-1})	k_{nr} (10^4 s^{-1})
1	Ru ^a	Ph	ⁱ Pr-DAB	495	633	5.3	2.6	1.5	0.55	0.37
2	Ru	Ph	pAn-DAB	552	767	5.0	0.72			
3	Ru	Ph	pAn-BIAN	595	821	4.6	0.68			
4	Ru	Ph	dmb	495	604	3.6	11	5.7	0.62	0.10
5	Ru	Me	ⁱ Pr-DAB	507	733	6.1	0.62			
6	Ru	Me	dmb	567	736	4.0	0.60			
7	Os	Ph	ⁱ Pr-DAB	478	655	5.7	0.32	0.58	1.8	3.13
8	Os	Ph	dmb	485	589	3.6	2.3	3.4	1.5	0.42
9	Os	Me	ⁱ Pr-DAB	478	714	6.9	0.16			
$[\text{Ru}(\text{Cl})(\text{Me})(\text{CO})_2(^i\text{Pr-DAB})]^b$				387	650	10	0.003	0.034	11	384

^a From ref 8. ^b From ref 47.

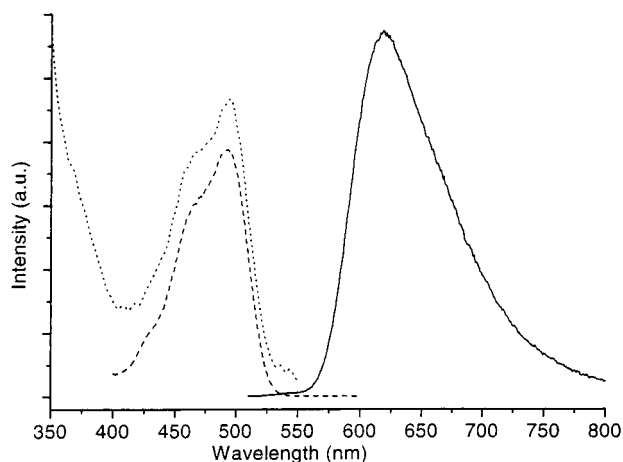


Figure 4. Emission spectrum (solid line, $\lambda_{\text{exc}} = 500 \text{ nm}$), excitation spectrum (dashed line, $\lambda_{\text{em}} = 620 \text{ nm}$), and ground-state absorption spectrum (dotted line) of $[\text{Ru}(\text{SnPh}_3)_2(\text{CO})_2(\text{dmb})]$ in a 2-MeTHF glass at 90 K.

account a difference in emission energy, both emissions most likely belong to the same excited state of the complex in a different environment or isomeric form. The former explanation was given in the case of $[\text{Re}(\text{SnPh}_3)(\text{CO})_3(\text{bpy})]$ because the effect was not observed for this complex in its solid state.²⁵ Variable excitation wavelength time-resolved emission measurements, using a continuously tuneable Coherent Infinity XPO laser, showed that both the emission maximum and lifetime are constant for excitation wavelengths covering most of the absorption band and only start to change at the extreme long-wavelength side of the absorption band.

Replacement of ruthenium by osmium has only a small effect on the absorption and emission energies of the $[M(\text{SnPh}_3)_2(\text{CO})_2(\alpha\text{-diimine})]$ complexes. Despite this, the emission lifetimes of the Os complexes are much shorter because of the increase of spin-orbit coupling (SOC) going from Ru to Os. For all complexes the quantum yields of emission (Table 3) from the ³SBLCT states are rather small in view of their very long emission lifetimes. In the next section we will discuss this observation and its consequences in more detail.

Discussion

The complexes under study belong to a group of α -diimine compounds in which two coligands are bound to the central metal atom via high-lying σ orbitals. These coligands may be alkyl groups or metal fragments. The lowest-energy transitions of these complexes are fundamentally different from those of complexes with only one such coligand., e.g., $[\text{Ru}(\text{Cl})(\text{R})(\text{CO})_2(\alpha\text{-diimine})]$ ¹⁷ or $[\text{Ru}(\text{Cl})(\text{SnPh}_3)(\text{CO})_2(\alpha\text{-diimine})]$.⁸ Transitions

from the $\sigma(\text{Ru-R})$ or $\sigma(\text{Ru-Sn})$ orbitals to $\pi^*(\alpha\text{-diimine})$ are normally not observed, and the lowest-energy transitions of these latter complexes have $d_\pi(\text{Ru}) \rightarrow \pi^*(\alpha\text{-diimine})$ (MLCT) character. This situation changes completely when two metal fragments are coordinated in an axial position to Ru (or Os), as in the case of $[M(\text{SnR}_3)_2(\text{CO})_2(\alpha\text{-diimine})]$, according to density functional (DFT) MO calculations on the model complex $[\text{Ru}(\text{SnH}_3)_2(\text{CO})_2(\text{H-DAB})]$.¹⁵ The HOMO, denoted as $\sigma(\text{Sn-Ru-Sn})$, consists of contributions from the antisymmetric combination of the Sn fragment σ orbitals $\text{Sn}(\text{sp}^3\text{-sp}^3)$ (42%) and from the Ru(5p) (15%) and H-DAB(π^*) (27%) orbitals. This implies a strong $\sigma\text{-}\pi^*$ interaction, i.e., a large delocalization of electron density from the Sn-Ru-Sn σ bond over the H-DAB ligand. According to the calculations, the LUMO of the model complex is also delocalized because it has contributions from H-DAB(π^*) (61%), Ru($4d_{yz}$) (11%), and Sn($\text{sp}^3\text{-sp}^3$) (27%). The $\sigma(\text{Sn-M-Sn}) \rightarrow \pi^*(\alpha\text{-diimine})$ transition between the HOMO and LUMO is strongly allowed. In view of the nature of the orbitals involved, this transition is called sigma-bond-to-ligand charge transfer.²⁶ Because of the strong $\sigma\text{-}\pi^*$ interaction, the lowest-energy (SBLCT) transitions of the complexes under study are less solvatochromic than the MLCT transition of the isostructural complex $[\text{Ru}(\text{Cl})(\text{Me})(\text{CO})_2(^i\text{Pr-DAB})]$ (see Table 1). The population of $\pi^*(^i\text{Pr-DAB})$ in the ground state, due to the strong $\sigma\text{-}\pi^*$ interaction, causes a lengthening of the CN bond and a shortening of the CC bond because the lowest π^* orbital of an α -diimine such as ⁱPr-DAB is antibonding between the N and C atoms of the $\text{N}=\text{C}-\text{C}=\text{N}$ skeleton and is bonding between the central C atoms. This is evident from the crystal structure of $[\text{Ru}(\text{SnPh}_3)_2(\text{CO})_2(^i\text{Pr-DAB})]$ in which CN and CC bond lengths of 1.34 and 1.39 Å, respectively, were found. This indicates much more $\sigma\text{-}\pi^*$ interaction than for $[\text{Ru}(\text{I})(\text{Me})(\text{CO})_2(^i\text{Pr-DAB})]$ having CN and CC bond lengths of 1.26 and 1.48 Å, respectively. As can be seen from Table 1, the absorption bands of the R-DAB and pAn-BIAN complexes are less solvatochromic than those of the aromatic dmb compounds. This means that the σ and π^* orbitals of the dmb complexes have less interaction and, accordingly, their $\sigma(\text{Sn-M-Sn}) \rightarrow \pi^*(\alpha\text{-diimine})$ (M = Ru, Os) transitions have more charge-transfer character. The strong $\sigma\text{-}\pi^*$ interaction of the R-DAB complexes causes the SBLCT transition to occur at higher energy than expected on the basis of its π^* -orbital energy. This effect becomes evident when the SnPh₃ is replaced by the more electron-donating SnMe₃ in the complexes $[\text{Ru}(\text{SnR}_3)_2(\text{CO})_2(\alpha\text{-diimine})]$ (R = Ph, Me; α -diimine = ⁱPr-DAB, dmb) (Table 1). A red shift of the absorption band is then observed in the case of the dmb complexes but not for the ⁱPr-DAB compounds.

(26) Djurovich, P. I.; Watts, R. J. *Inorg. Chem.* **1993**, *32*, 4681.

The differences between the [M(SnPh₃)₂(CO)₂(α-diimine)] complexes possessing a low-energy SBLCT transition and the isostructural complex [Ru(Cl)(Me)(CO)₂(ⁱPr-DAB)] having a lowest MLCT transition are not reflected in the absorption spectra but become evident when their resonance Raman spectra and especially their photophysical and photochemical behavior are compared. The main difference is the observation of rather strong rR effects for a few vibrations in the case of [Ru(Cl)(Me)(CO)₂(ⁱPr-DAB)] and weak rR effects for many vibrations in the case of the [M(SnR₃)₂(CO)₂(ⁱPr-DAB)] complexes. The latter observation confirms the delocalized character of the SBLCT transition during which many bonds are only weakly distorted in the excited state. This weakness of distortion is also demonstrated by the emission spectra (vide infra). The rR spectra of [Ru(SnPh₃)₂(CO)₂(ⁱPr-DAB)] (which is taken as a representative for all the [M(SnR₃)₂(CO)₂(ⁱPr-DAB)] complexes) show strong rR effects for bands at 1473, 1283, 953, and 836 cm⁻¹, while ν_s(CO) is not observed at all. The absence of ν_s(CO) implies that the charge density at the central metal atom is hardly affected by the electronic transition. This result agrees with the main conclusion from the DFT calculations on the model complex [Ru(SnH₃)₂(CO)₂(H-DAB)] that the central metal atom and the carbonyls are hardly involved in the σ → π* (SBLCT) transition.¹⁵ The rR band at 1473 cm⁻¹ is assigned to ν_s(CN), which is lower in frequency than for [Ru(Cl)(Me)(CO)₂(ⁱPr-DAB)] (1568 cm⁻¹) because of the strong σ-π* interaction. The observation of a rR effect for a band at 1283 cm⁻¹ is exceptional. It has only been observed for complexes such as [W(CO)₄(R-DAB)] (R = *p*-tolyl, mesityl),²⁷ [Re{Re(CO)₅-(CO)₃(ⁱPr-DAB)}],²⁰ and [Ru(L₁)(L₂)(CO)₂(ⁱPr-DAB)] (L₁, L₂ = metal fragment)^{8,28,29} in which there is a very strong d_π-π* or σ-π* interaction (π-backbonding). According to preliminary calculations, it is a coupled δ_s(CH) + ν_s(CN) vibration in which δ_s(CH) is a symmetric in-plane deformation of the imine hydrogen atoms. This coupling, which is responsible for the resonance enhancement of this vibration, most probably occurs because of the small energy difference between these two local modes. In the case of [Ru(SnPh₃)₂(CO)₂(ⁱPr-DAB)] strong rR effects are also observed for deformation modes of ⁱPr-DAB at 953 and 836 cm⁻¹. Again, these vibrations are always observed when there is a strong d_π-π* or σ-π* interaction.^{8,27-29} The observation of ν(M-Sn) and δ(CH₃) (for the SnMe₃ complexes) indicates that the transition indeed occurs from a σ(Sn-M-Sn) orbital rather than from a d_π(M) orbital.

According to the TA spectra, the complexes [M(SnPh₃)₂(CO)₂(α-diimine)] have much longer excited-state lifetimes at room temperature (τ = 0.5–3.6 μs; Table 1) than [Ru(Cl)(Me)(CO)₂(ⁱPr-DAB)] (τ = 63 ns)³⁰ even though the former complexes are photolabile. This photolability, not observed for [Ru(Cl)(Me)(CO)₂(ⁱPr-DAB)], is a specific property of complexes having a lowest SBLCT state and involves a homolytic splitting of a M-Sn bond from this state.³¹ Because of this photolability, the ³SBLCT states of [Ru(SnPh₃)₂(CO)₂(dmb)] and [Ru(SnPh₃)₂(CO)₂(ⁱPr-DAB)] have coincidentally the same

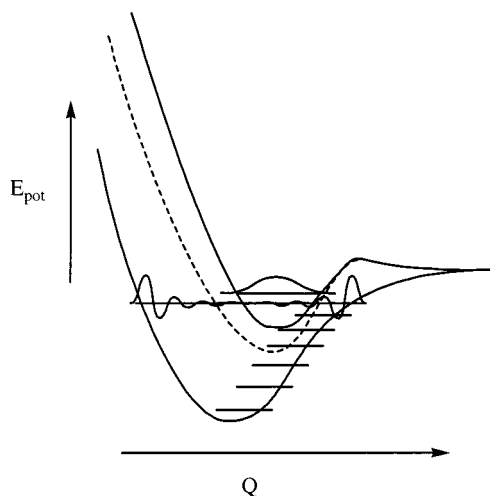


Figure 5. Qualitative potential energy curves of ground and excited states of [Ru(SnPh₃)₂(CO)₂(ⁱPr-DAB)] (solid line) and [Ru(SnPh₃)₂(CO)₂(pAn-DAB)] (dotted line).

lifetimes (Table 1) although the dmb ligand is much more rigid and the ³SBLCT state of its complex is at somewhat higher energy (Table 3). The large influence of the photoreactivity on the excited-state lifetime also becomes evident when the ⁱPr-DAB ligand is replaced by an α-diimine with a lower-lying π* orbital such as pAn-DAB or pAn-BIAN. The SBLCT states are then lower in energy, and although the energy gap law (EGL) predicts a decrease of excited-state lifetime, this lifetime becomes much longer because of the larger photostability (Table 1). For instance, the quantum yield for the photoreaction of the [Ru(SnPh₃)₂(CO)₂(R-DAB)] complexes in CH₂Cl₂ at room temperature is 0.10 for R = ⁱPr but only 0.006 for R = pAn. This increase of photostability is most probably due to an increase of the barrier for this reaction, as clarified in Figure 5 by the qualitative potential curves for ground and ³SBLCT states of the [Ru(SnPh₃)₂(CO)₂(R-DAB)] (R = ⁱPr, pAn) complexes. Because the Os-Sn bonds are stronger than the Ru-Sn bonds, the [Os(SnPh₃)₂(CO)₂(α-diimine)] complexes are more photostable than the Ru ones (e.g., Φ = 0.038 for [Os(SnPh₃)₂(CO)₂(ⁱPr-DAB)] and Φ = 0.10 for its Ru analogue). As a result, their SBLCT states are also longer-lived than those of the Ru compounds, despite the larger spin-orbit coupling constant of the Os atom. Because of their photostability, the lifetimes of the Os complexes at room temperature also increase when ⁱPr-DAB is replaced by dmb, i.e., when the α-diimine becomes more rigid (Table 1).

The differences between the ³SBLCT states of the [M(SnPh₃)₂(CO)₂(α-diimine)] complexes and the ³MLCT state of [Ru(Cl)(Me)(CO)₂(ⁱPr-DAB)] become even more pronounced at low temperature, under which conditions all complexes are photostable. The emitting ³SBLCT states of the [M(SnR₃)₂(CO)₂(α-diimine)] complexes are much longer-lived than the ³MLCT state of [Ru(Cl)(Me)(CO)₂(ⁱPr-DAB)], an effect that was already noted for the complex [Ru(SnPh₃)₂(CO)₂(ⁱPr-DAB)].⁸ This increase of lifetime is caused by a decrease of distortion of the complexes in their lowest excited state, which is reflected in a decrease of the apparent Stokes shift (i.e., the energy difference between the absorption and emission maxima, ΔE_{abs-em}; see Table 3) from 10 × 10³ cm⁻¹ to (3.5–6.0) × 10³ cm⁻¹ going from [Ru(Cl)(Me)(CO)₂(ⁱPr-DAB)] to [M(SnR₃)₂(CO)₂(α-diimine)]. This implies that for the ³SBLCT state the potential energy curve is shifted less with respect to that of the ground state and that the vibrational overlap between these curves is

(27) Balk, R. W.; Stufkens, D. J.; Oskam, A. *J. Chem. Soc., Dalton Trans.* **1982**, 275.

(28) Aarnts, M. P.; Wilms, M. P.; Stufkens, D. J.; Baerends, E. J.; Vlček, A., Jr., *Organometallics* **1997**, *16*, 2055.

(29) Van Slageren, J.; Hartl, F.; Stufkens, D. J. *Eur. J. Inorg. Chem.* **2000**, 847.

(30) Nieuwenhuis, H. A.; Stufkens, D. J.; McNicholl, R. A.; Al-Obaidi, A. H. R.; Coates, C. G.; Bell, S. E. J.; McGarvey, J. J.; Westwell, J.; George, M. W.; Turner, J. J. *J. Am. Chem. Soc.* **1995**, *117*, 5579.

(31) Aarnts, M. P.; Stufkens, D. J.; Vlček, A., Jr. *Inorg. Chim. Acta* **1997**, *266*, 37.

smaller for $[\text{M}(\text{SnPh}_3)_2(\text{CO})_2(\text{Pr-DAB})]$ than for $[\text{Ru}(\text{Cl})(\text{Me})(\text{CO})_2(\text{Pr-DAB})]$,^{32–34} causing a decrease of the rate constant for nonradiative decay k_{nr} (EGL effect). In fact, k_{nr} decreases by a factor of 1000 going from $[\text{Ru}(\text{Cl})(\text{Me})(\text{CO})_2(\text{Pr-DAB})]$ to $[\text{Ru}(\text{SnPh}_3)_2(\text{CO})_2(\text{Pr-DAB})]$ (Table 3) even though the emission energy hardly changes. Correspondingly, the emission lifetime, which is mainly determined by k_{nr} , increases by a factor of ca. 1000 from 0.30 to $2.6 \times 10^2 \mu\text{s}$. This increase of vibrational overlap with an increase of distortion is clear from Figure 5. The overlap is minimal if the equilibrium distance is the same in the ground and excited states but increases dramatically if there is an appreciable lengthening of this distance in the excited state.

If an R-DAB ligand is replaced by pAn-BIAN and finally by a fully aromatic ligand, the α -diimine becomes more rigid. The complex is then even less distorted in its excited state, and this results in a smaller apparent Stokes shift, a smaller value of k_{nr} , and a longer emission lifetime. Of course, part of the decrease of k_{nr} is caused by the fact that the dmb complex emits at somewhat higher energy. The rigidity of the dmb ligand, combined with the specific properties of the ³SBLCT state, causes the complex $[\text{Ru}(\text{SnPh}_3)_2(\text{CO})_2(\text{dmb})]$ to have an extremely long emission lifetime of 1.1 ms in a glass at 90 K. Emission lifetimes this long are virtually unknown for charge-transfer states of organometallic compounds. Various other types of long-lived excited states are known, and they all feature a diminished involvement of the transition metal atom in the excited state. Thus, for Ru(II) α -diimine complexes in which a low-lying intraligand (IL) state interacts with the MLCT state, the excited-state lifetime may increase by 2 orders of magnitude. An example is $[\text{Ru}(\text{bpy-pyr})(\text{bpy})_2]^{2+}$; a $[\text{Ru}(\text{bpy})_3]^{2+}$ type complex in which one bpy ligand has been functionalized with a pyrene group. In this case the MLCT emission decay is biexponential, the longer-lived component ($\tau = 50 \mu\text{s}$ at room temperature) being due to internal conversion from the higher-lying pyrene ³IL state to the ³MLCT state.³⁵ When an ethynyl group is inserted between the bpy and pyrene units, the IL and MLCT states are in thermal equilibrium, leading to a single-exponential decay with a lifetime of 46 μs .³⁶ An even longer excited-state lifetime was found for $[\text{Ru}(\text{CN}_2\text{-np})(\text{bpy})_2]^{2+}$ (CN₂-np = naphtho[2,3-*f*][1,*o*]phenanthroline-9,14-dicarbonitrile); $\tau = 464 \mu\text{s}$ at 77 K.³⁷ Excited states that are virtually purely IL in character can have even longer lifetimes. Examples include various metalloporphyrins³⁸ and the complexes $[\text{M}(\text{bpy})_3]^{3+}$ (M = Rh, Ir).^{39,40} Ligand-to-ligand charge transfer (L'LCT) states, among which the SBLCT states may be reckoned in view of the limited involvement of the transition metal, can be long-lived as well.⁴¹ In the L'LCT state of $[\text{Zn}(4\text{-Cl-PhS})_2(\text{phen})]$ negative charge has been transferred from the thiolate donors to the phenanthroline acceptor. The lifetime of this ³L'LCT state

is 8 ms at 6.5 K.⁴² For analogous transition metal complexes the excited-state lifetime is shorter, e.g., $\tau = 6.1 \mu\text{s}$ for $[\text{Pt}(\text{bpy})(\text{mnt})]$ (mnt = maleonitriledithiolate) in the solid state at 77 K.

Replacement of ruthenium by osmium has only a small effect on the absorption and emission energies of the $[\text{M}(\text{SnPh}_3)_2(\text{CO})_2(\alpha\text{-diimine})]$ complexes. Thus, the energy of the ³SBLCT state hardly varies with M. Despite this, the excited-state lifetime is much shorter because of an increase in spin-orbit coupling. In contrast to this, MLCT states show a decrease of both the emission energy and lifetime when Ru is replaced by Os. For instance, the complex $[\text{Ru}(\text{bpy})_3]\text{Cl}_2$ emits in a 77 K ethanol/methanol glass at 584 nm with a lifetime of 5.3 μs , while $[\text{Os}(\text{bpy})_3]\text{Cl}_2$ emits at 710/773 nm with a lifetime of 0.83 μs under these circumstances.⁴³ Complexes with a lowest IL state also show a decrease of excited-state lifetime going from a second- to a third-row transition metal. For instance, the excited-state lifetime of $[\text{M}(\text{bpy})_3]^{3+}$ is 2.2 ms for M = Rh³⁹ but is only 0.080 ms for M = Ir.⁴⁰ Likewise, the excited-state lifetime of $[\text{M}(\text{TPP})]$ (TPP = tetraphenylporphyrine) is 2800 μs for M = Pd and 291 μs for M = Pt.³⁸

For all complexes under study the quantum yields of emission Φ_{em} from the ³SBLCT state are rather small in view of their very long emission lifetimes. By use of the equation $\Phi_{\text{em}}/\tau = \Phi_{\text{isc}}k_{\text{r}}$, values are obtained for $\Phi_{\text{isc}}k_{\text{r}}$ that do not exceed $1.8 \times 10^2 \text{ s}^{-1}$ (Table 3). In fact, these values are much lower than that found for the isostructural complex $[\text{Ru}(\text{Cl})(\text{Me})(\text{CO})_2(\text{Pr-DAB})]$ ($\Phi_{\text{isc}}k_{\text{r}} = 11 \times 10^2 \text{ s}^{-1}$) having a lowest ³MLCT excited state. In general, ³MLCT states have radiative decay constants k_{r} that are even higher and range between 10^4 and 10^5 s^{-1} .³⁵ These low values of $\Phi_{\text{isc}}k_{\text{r}}$ for the emission from the ³SBLCT state are rather unexpected because the electronic transition to the corresponding ¹SBLCT state is strongly allowed ($\epsilon = (3-15) \times 10^3 \text{ M}^{-1} \text{ cm}^{-1}$; Table 1). The values of $\Phi_{\text{isc}}k_{\text{r}}$ and of the emission quantum yields are therefore not lower than expected because k_{r} is small but because Φ_{isc} is much smaller than unity. Lower values of Φ_{isc} are obtained if crossing between ¹SBLCT and ³SBLCT is slow or if there is a competing intersystem crossing from the ¹SBLCT state to another nonemitting state of ³MLCT character. According to recent CASSCF/CASPT2 calculations of the ground state and some singlet and triplet-excited states of the model complex $[\text{Ru}(\text{SnH}_3)_2(\text{CO})_2(\text{Me-DAB})]$,⁴⁴ both factors may play an important role here. Thus, the calculated energy difference between the ¹SBLCT and ³SBLCT states of 5400 cm^{-1} is rather high compared with that between the lowest ¹MLCT and ³MLCT states (1500 cm^{-1}). This high-energy difference may cause a slowing down of the intersystem crossing to such an extent that fluorescence from the ¹SBLCT state can compete with this process. In fact a short-lived and only slightly Stokes shifted emission was observed, most probably belonging to fluorescence from the ¹SBLCT state.^{6,8} This luminescence, which is not due to fluorescence from solvent impurities or any other artifact, has a lifetime of 800 ps for $[\text{Ru}(\text{SnPh}_3)_2(\text{CO})_2(\text{Pr-DAB})]$ in a 2-MeTHF glass at 90 K. This lifetime was determined with a Hamamatsu streak camera setup,⁴⁵ using a nitrogen laser ($\lambda_{\text{exc}} = 337 \text{ nm}$) as the excitation source.

(32) Damrauer, N. H.; Boussie, T. R.; Devenney, M.; McCusker, J. K. *J. Am. Chem. Soc.* **1997**, *119*, 8253.

(33) Treadway, J. A.; Loeb, B.; Lopez, R.; Anderson, P. A.; Keene, F. R.; Meyer, T. *J. Inorg. Chem.* **1996**, *35*, 2242.

(34) Strouse, G. F.; Schoonover, J. R.; Duesing, R.; Boyde, S.; Jones, W. E., Jr.; Meyer, T. *J. Inorg. Chem.* **1995**, *34*, 473.

(35) Baba, A. I.; Shaw, J. R.; Simon, J. A.; Thummel, R. P.; Schmehl, R. H. *Coord. Chem. Rev.* **1998**, *171*, 43.

(36) Harriman, A.; Hissler, M.; Khatyr, A.; Ziessel, R. *Chem. Commun.* **1999**, 735.

(37) Albano, G.; Belsler, P.; Cola, L. D.; Gandolfi, M. T. *J. Chem. Soc., Chem. Commun.* **1999**, 1171.

(38) Eastwood, D.; Gouterman, M. *J. Mol. Spectrosc.* **1970**, *35*, 359.

(39) DeArmond, M. K.; Hillis, J. E. *J. Chem. Phys.* **1971**, *54*, 2247.

(40) Flynn, C. M., Jr.; Demas, D. M. *J. Am. Chem. Soc.* **1974**, *96*, 1959.

(41) Vogler, A.; Kunkely, H. *Comments Inorg. Chem.* **1990**, *9*, 201.

(42) Kotal, C. *Coord. Chem. Rev.* **1990**, *99*, 213.

(43) Fabian, R. H.; Klassen, D. M.; Sonntag, R. W. *Inorg. Chem.* **1980**, *19*, 1977.

(44) Turki, M.; Daniel, C. 34th International Conference on Coordination Compounds, Edinburgh July 8–14, 2000. *Coord. Chem. Rev.*, to be published.

(45) Lauteslager, X. Y.; van Stokkum, I. H. M.; van Ramesdonk, H. J.; Brouwer, A. M.; Verhoeven, J. W. *J. Phys. Chem. A* **1999**, *103*, 653.

A second noteworthy result of the CASSCF/CASPT2 calculations is the presence of a ³MLCT state very close in energy to the absorbing ¹SBLCT state. Intersystem crossing to this ³MLCT state will compete with decay to the ³SBLCT state, the more because crossing between ¹SBLCT and ³MLCT has been found to be much more efficient than between ¹SBLCT and ³SBLCT states.⁴⁶ Moreover, occupation of the ³MLCT state in question is not expected to give rise to any strong additional emission because the electronic transition to the corresponding ¹MLCT state, observed as a weak band at ca. 400 nm in the case of [Ru(SnPh₃)₂(CO)₂(ⁱPr-DAB)], is overlap-forbidden.

We therefore propose that the low emission quantum yields of the complexes under study are the result of two effects, i.e., the large energy gap between the ¹SBLCT and ³SBLCT states and the presence of a nonemissive ³MLCT state close in energy to the ¹SBLCT state.

(46) Daniel, C.; Guillaumont, D.; Ribbing, C.; Minaev, B. *J. Phys. Chem. A* **1999**, *103*, 5766.

(47) Nieuwenhuis, H. A.; Stufkens, D. J.; Vlček, A., Jr. *Inorg. Chem.* **1995**, *34*, 3879.

Conclusions

The results of this study show that the photostability of these complexes at room temperature can be increased appreciably by using an α -diimine with a low-lying π^* orbital and osmium instead of ruthenium. In this way virtually photostable complexes were prepared with lifetimes of ca. 4 μ s. In a glass at 80 K all complexes are photostable, and because the complexes are only weakly distorted in their emitting ³SBLCT states according to the Stokes shift and resonance Raman spectra, extremely long emission lifetimes of up to 1 ms were obtained. Ab initio calculations suggest that this may be due to an inefficient decay to the emitting ³SBLCT state, but this will be investigated further by ultrafast time-resolved absorption studies.

Acknowledgment. Many thanks are due to Dr. C. Daniel (CNRS, Strasbourg) for very fruitful discussions and for providing us with the theoretical data of [Ru(SnH₃)₂(CO)₂(Me-DAB)] before publication.

IC000857X